Model of the Kinetics of Polymorphous Crystallization

B. Morin,[1] K. R. Elder,[1,2] M. Sutton,[1] and Martin Grant[1]

[1]*Physics Department, McGill University, Rutherford Building, 3600 rue University, Montréal, Québec, Canada H3A 2T8*

[2]*Department of Physics and Materials Research Laboratory, University of Illinois at Urbana-Champaign, 1110 West Green Street, Urbana, Illinois 61801*

(Received 22 March 1995)

We propose a phase-field model for the kinetics of isothermal crystallization of an amorphous solid at a concentration nearly equal to the equilibrium crystal stochiometry. The model utilizes two coupled fields: a nonconserved ordering vector field which describes the local lattice structure and a conserved nonordering scalar field describing the local atomic composition. Results of large-scale computer simulations are reported which can be compared with experiments.

PACS numbers: 61.50.Cj, 64.60.My

The isothermal crystallization of a liquid or amorphous material is mediated through the nucleation and growth of small crystallites. The emerging regular crystal structure that defines the crystallites is obtained through a rearrangement of the local atomic composition. Even in the absence of elastic effects this implies a subtle coupling between the local crystal structure and composition. Motivated by the possibility of making simultaneous measurements of the crystallization kinetics (i.e., the development of Bragg peaks in large angle x-ray scattering) and the compositional reequilibration (i.e., through small-angle x-ray scattering), and by preliminary reports of such measurements [1], we have developed a nonlinear field theory to describe these phenomena [2]. A large-scale numerical analysis of this model is used to study the crystallization process and can be compared to experiment.

We consider isothermal crystallization at a concentration nearly equal to the equilibrium crystal stoichiometry, that is, polymorphic crystallization. Our model involves two coupled stochastic fields, and is related to previous work on order-disorder transitions [3] and to model C of critical dynamics [4]. The local crystalline order is modeled by a d-component nonconserved vector field $\vec{\psi}(\mathbf{x}, t)$ of space $\mathbf{x}$ and time t. The local crystal orientation is represented by the direction of $\vec{\psi}$, while the magnitude of $\vec{\psi}$ determines the relative order of the system. The free energy is an analytic function of the fields, and the isotropy of the disordered state implies that the potential density should be an $O(d)$-symmetric function of the ordering field, i.e., $\mathcal{V}(\vec{\psi}) = f(|\vec{\psi}|^2)$. Since crystallization is a first-order phase transition, f must be expanded to at least $(|\vec{\psi}|^2)^3$. The continuous symmetry of this energy is unrealistic for samples with many crystallites (i.e., polycrystalline), since grain boundaries or domain walls (due to lattice mismatch) always exist between neighboring crystallites. Thus an explicit symmetry breaking term must be added to suppress the "spin waves" [5] associated with $O(d)$ systems.

The other field, $c(\mathbf{x}, t)$, is a scalar globally conserved field which represents the local atomic composition of the binary alloy [3]. Since, in equilibrium, the crystal orientation is independent of the local atomic composition, c is a nonordering field which couples symmetrically to the ordering field. In the model, no variation in density between the two phases is described, except for that controlled by concentration variation.

These considerations lead to a free energy functional $F = F_1[\vec{\psi}] + F_2[\vec{\psi}, c]$, where

$$F_1[\vec{\psi}] = \int d\mathbf{x}\Big[\frac{\kappa}{2}|\nabla\vec{\psi}(\mathbf{x})|^2 + \frac{r}{2}|\vec{\psi}(\mathbf{x})|^2 + \frac{v}{6}[|\vec{\psi}(\mathbf{x})|^2]^3 - \frac{s}{4}\frac{1 + b\cos[n\theta(\mathbf{x})]}{1 + b}[|\vec{\psi}(\mathbf{x})|^2]^2\Big] \quad (1)$$

and

$$F_2[\vec{\psi}, c] = \int d\mathbf{x}\Big[\frac{\beta}{2}|\nabla c(\mathbf{x})|^2 + \frac{w}{2}c(\mathbf{x})^2 + \frac{\alpha}{2}c(\mathbf{x})|\vec{\psi}(\mathbf{x})|^2\Big]. \quad (2)$$

The term $\cos[n\theta(\mathbf{x})]$ breaks the rotational symmetry of the ordered state by introducing n wells in θ, which is somewhat analogous to the Z_n model [6], but with an important difference, explained below. Here $\cos\theta = \hat{x}\cdot\vec{\psi}/|\vec{\psi}|$, and $\hat{x}$ is a constant unit vector. The size of the parameter b dictates the type of domain walls which forms. For small values of b, it is energetically favorable for the ordering field to jump between neighboring orientations at constant $|\vec{\psi}|$, thereby mimicking a grain boundary with only a lattice mismatch. For large values of b it is favorable for the magnitude of $\vec{\psi}$ to decrease at a grain boundary, corresponding to amorphous material trapped at the boundary.

For the simpler case of order-disorder transitions [3,7] the coupling parameter α is explicitly a function of the average concentration and goes to zero at or near perfect stoichiometry. This coupling leads to concentration fluctuations at antiphase domain boundaries during the ordering process. The physical interpretation of this result is

 0031-9007/95/75(11)/2156(4)$06.00

that the system attempts to order at the ideal stoichiometry by pushing any excess concentration to the antiphase domain walls. The coupling has a similar influence in the present model, with a subtle difference; the amount of concentration pushed to a domain wall depends on the relative orientation of the neighboring crystallites and the size of crystallites. This is the essential difference from the Z_n model and it leads to interesting results, to be discussed later.

In equilibrium, the concentration field can be conveniently integrated out giving rise to the free energy functional $F'[\psi] = F_1[\psi] + F_2'[\psi]$, with $F_2'[\vec{\psi}] = (-\alpha^2/8w) \int d\mathbf{x} \int d\mathbf{x}' |\vec{\psi}(\mathbf{x})|^2 \mathcal{U}(|\mathbf{x} - \mathbf{x}'|) |\vec{\psi}(\mathbf{x}')|^2$, where F' determines the equilibrium probability distribution of $\vec{\psi}$. In Fourier space, the nonlocal coupling $\mathcal{U}(x)$ has the form $\hat{\mathcal{U}}(q) = 1/(q^2 + w/\beta)$, except at $q = 0$ where $\hat{\mathcal{U}}(q) = 0$. Nonlocality becomes important for $\sqrt{\beta/w} \geq \xi \simeq \sqrt{\kappa/r}$, where ξ is the correlation length associated with the ordering field.

Mean-field expressions for the domain-wall energy can be straightforwardly obtained in $d = 2$. Indeed, most of our detailed analyses are for two dimensions, but we expect qualitatively the same results in three dimensions. Writing $\vec{\psi}(\mathbf{x})$ in polar coordinates, i.e., $\vec{\psi} = R[\hat{x} \cos(\theta) + \hat{y} \sin(\theta)]$, and minimizing F' with respect to $\theta(\mathbf{x})$ and $R(\mathbf{x})$, gives the mean-field interface equations. These represent lattice mismatch between neighboring crystallites with surface tension σ_θ and amorphous material trapped within domain walls with a tension σ_R. The surface tension is defined to be $\sigma = \kappa \int_{-\infty}^{\infty} dx |\partial_x \vec{\psi}_0(x)|^2/2$, where $\vec{\psi}_0(x)$ corresponds to a minima of the free energy with boundary conditions fixed at $x = \pm\infty$. The boundary conditions which determine σ_R and σ_θ are $[\vec{\psi}(-\infty), \vec{\psi}(\infty)] = [R\hat{x}, -R\hat{x}]$ and $[\vec{\psi}(-\infty), \vec{\psi}(\infty)] = [R\hat{x}, R(\hat{x} \sin(2\pi/n) + \hat{y} \cos(2\pi/n))]$, respectively, where $\vec{\psi} = \pm R\hat{x}$ is a minima of F. It is straightforward to obtain these surface tensions near the first-order transition point (i.e., $s^2 = 16r/3$), in the limit that the nonlocal interaction can be ignored (i.e., $s \gg \alpha^2/2w$). For convenience v is set to unity. The energies per unit area are $\sigma_\theta = (2R^3/n)\sqrt{\kappa s b/(1 + b)}$ and $\sigma_R = (3s^2/128)\sqrt{3\kappa}$. For $n \to \infty$, the miscibility gap between neighboring minima goes to zero, and $\sigma_\theta \to 0$. For $n = 2$ the model essentially reduces to model C [3,4]. For the simulations to follow, the parameters were chosen such that the ratio σ_θ/σ_R is approximately 0.8, implying that interface solutions involve paths which go from one global minima of the effective potential to another by varying R but without entering the center well.

When the system is brought out of equilibrium, it evolves into its new equilibrium state according to Langevin equations, whose form is dictated by the free energy and by conservation laws, namely,

$$\partial \vec{\psi}/\partial t = -\Gamma \, \delta F/\vec{\delta} \psi + \vec{\eta}_\psi \tag{3}$$

and

$$\partial c/\partial t = D \nabla^2 \delta F/\delta c + \eta_c , \tag{4}$$

where the functional derivatives ensure that the free energy is minimized in equilibrium. Γ is a mobility, D is a diffusion constant, and the random noises η have intensities proportional to the temperature T as determined by fluctuation-dissipation relations [4]. Equation (4) can be solved in the long time limit [7] giving

$$c(\mathbf{q}, t) \approx e^{\gamma t} c(\mathbf{q}, 0) + \int_0^t dt' e^{\gamma(t-t')} \eta_c(\mathbf{q}, t') + \frac{\alpha(e^{\gamma t} - 1)}{2(w + \beta q^2)} \int d\mathbf{x} e^{i\vec{q}\cdot\mathbf{x}} |\vec{\psi}(\mathbf{x}, t)|^2, \tag{5}$$

where $\gamma \equiv -Dq^2(w + \beta q^2)$. The first two terms in this expression describe the rapid reequilibration to the new metastable state. The last term indicates that c is slaved to the dynamics of $\vec{\psi}$. For $n = 2$, an approximate solution for ψ can be used to solve for the concentration correlation function $S_c(q, t) \equiv \langle |c(q, t)|^2 \rangle$. This calculations shows that, for large q, $S_c(q, t) \propto 1/q^{d-1}$, which is due to concentration fluctuations at the interfaces. For the present model the difference in domain wall energies leads to varying concentrations being collected at domain walls. Since c is a conserved field, the average concentration left behind in each crystallite varies. This effect is not present if all domain walls have the same energy, as, for example, in the case of the Z_n model mentioned earlier. The variation in c from crystallite to crystallite should lead to "Porod tails" [8], i.e., $S_c(q, t) \propto 1/q^{d+1}$ for large q. Indeed, the effect of variations in c both between crystallites and at domain walls leads to both $1/q^{d+1}$ and $1/q^{d-1}$ behavior, as we shall see below.

Equations (3) and (4) were numerically integrated in two dimensions. Euler's method was used for the time derivative, and central difference formulas were used for the spatial derivatives on a square lattice of N sites, with periodic boundary conditions. For these simulations the dimensionless parameters [9] were set to unity with the following exceptions: $(s, \alpha, \beta, T, b, \Delta t, N, n) = (4, 0.1, 0.25, 0.0016, 2, 0.01, 256^2, 12)$. The system was initially prepared in a disordered state and quenched below the first-order transition point where the amorphous state is metastable. Runs for 50 independent realizations of the initial conditions were averaged. Immediately following the quench, the system equilibrates in the metastable amorphous state, before the nucleation and growth of crystallites begin. The nucleation rate can be approximated [10] by $I \propto V \exp -\Delta F_c/T$, where ΔF_c is the activation energy of a critical droplet, V is the volume of phase space available for nucleation, and temperature is in energy units. Using the simulation parameters yields a negligible nucleation rate $I \sim 10^{-16}$ because the volume of phase space is small. While the rate can be increased by tuning the parameters so that there are large fluctuations in the ordered state or the system is close

to a point of spinodal ordering, it is more useful and faithful to experiments to incorporate a nucleation rate of $I = 1/40$, wherein seeds of fixed critical size were randomly introduced in space and time in such a way as to mimic homogeneous nucleation.

Figure 1 shows the typical evolution of configurations as crystallites form, grow, and coalesce. The magnitude of the ordering field (i.e., $|\vec{\psi}|$) is imaged on the left, while on the right the local concentration is shown. The concentration field does not phase separate, and can be seen to be slaved to the ordering field as suggested by Eq. (5). Concentration fluctuations can be discerned on the gray-scale image Fig. 1. The concentration within various crystallites reveals relative variations comparable to the average composition. These variations are the origin of the Porod tail in $S_c(q,t)$ (see below).

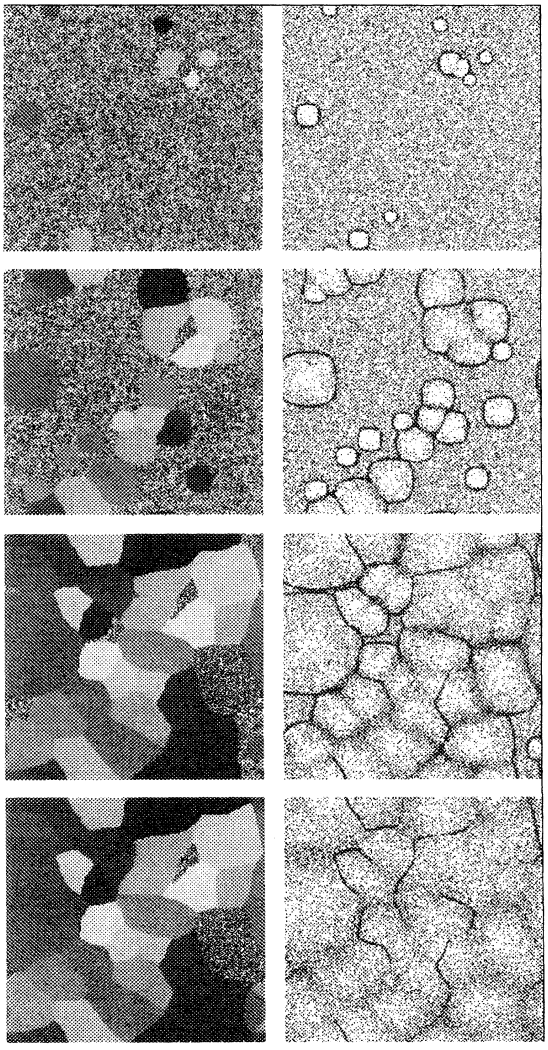

FIG. 1. Two parallel sets of configurations imaging the local magnitude of order parameter $|\vec{\psi}|$ (left) and the local concentration c (right) as a function of time $t = 8$, 24, 48, 80, from top to bottom. Gray scale of concentration shows weak step function in bulk crystallites due to differences in domain-wall energy. Also note the large concentration differences at different types of domain walls.

In Fig. 2, the structure factor for the concentration field is displayed. $S_c(q,t)$ shows both Porod behavior (i.e., $S_c \sim 1/q^{d+1}$ for intermediate wave numbers) and $1/q^{d-1}$ behavior for large wave numbers as is shown in the inset. In the same figure, the structure factor for the field corresponding to crystalline ordering $S_\psi(q,t) \equiv \langle \vec{\psi}^*(\mathbf{q},t) \cdot \vec{\psi}(\mathbf{q},t) \rangle = \langle |\vec{\psi}(\mathbf{q},t)|^2 \rangle$ is shown. The inset shows that S_ψ also has a Porod tail, due to the sharp domain walls between neighboring crystallites [11]. As expected, the tail appears in the range $1/\ell < q \ll 1/\xi$, where $\ell \approx 70$ is the average domain size and $\xi \approx 1$ is the correlation length.

Experimentally, small angle scattering is sensitive to the density fluctuations given by regions of different composition $[S_c(q,t)]$, and the high angle scattering is sensitive to the orientational distribution of crystallites $[S_\psi(q,t)]$. The small angle scattering is not sensitive to orientational order. If the composition is the same in every crystallite, as would be the case were c and ψ uncoupled, the small angle scattering should show $1/q^{d-1}$ tails. It is the coupling in the present model which gives the Porod tails $(1/q^{d+1})$, and we believe this is also the origin of those tails in the experimental observations. Care must be taken in each system to relate the scattering density (electron density for x rays and nuclear density

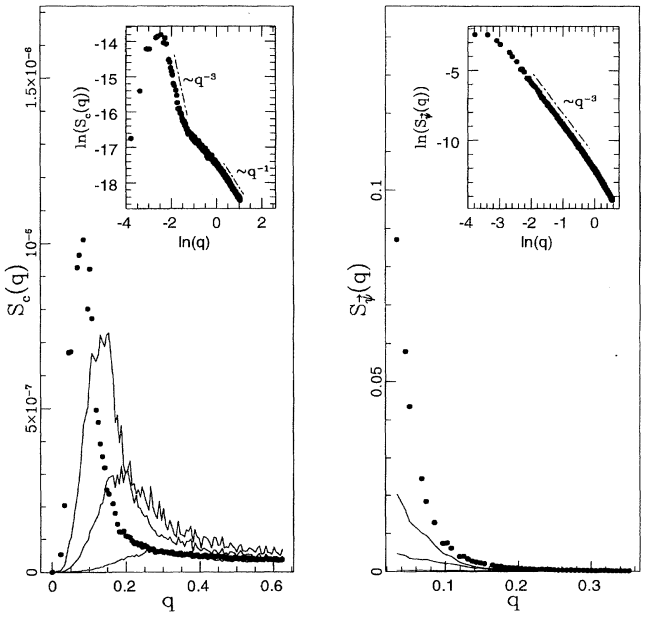

FIG. 2. Structure factors $S_c(q,t)$ (left) and $S_\psi(q,t)$ (right) as a function of wave number q, with times $t = 8$, 16, 24, 80 from bottom to top. Insets are ln-ln plots at $t = 80$ showing that *both* S_c and S_ψ have Porod tails $\sim 1/q^{d+1}$, where $d = 2$.

for neutrons) to the underlying variables (c and ψ in our simple model) controlling the transition.

In Fig. 3, the time evolution of S_c is shown for a few wave numbers. To improve statistics, several q's have been binned together. A two-step process is apparent. The concentration fluctuations of the prepared disordered state initially relax to a metastable state, followed by nucleation and growth. The initial relaxation is evident in the dependence of the fraction of ordered phase on time, shown in the inset: there is no visible nucleation for $t < 5$, whereas concentration fluctuations undergo rapid relaxation in that time interval. These kinetics are well fit by a standard Kolmogorov form [12], with an Avrami exponent corresponding to homogeneous nucleation. It is possible that initially a *decrease* in the structure factor may be observed instead of an increase. Such a situation arises either when metastable fluctuations are smaller than those of the initial state or simply from probing wave numbers greater than the inverse correlation length, $q > 1/\xi$. In either case, this initial relaxation is followed by the nucleation and growth of crystallites, as is evident in the fractional change of ordered phase. The resulting polycrystalline sample should, in principle, anneal to a single crystal, the final equilibrium state. This latter time scale is beyond the scope of this work, however.

To summarize, the three main conclusions following from our model are as follows: (I) The crystallization process occurs in three steps, a rapid relaxation in the metastable state, nucleation and growth of a polycrystalline sample, and finally the annealing of the polycrystalline sample; (II) $S_c(q,t)$ can show both $1/q^{d+1}$ and $1/q^{d-1}$ behaviors at intermediate and large q, respectively; (III) $S_{\vec{\psi}}$ has a Porod tail [11]. These results are experimentally accessible and are in qualitative agreement with preliminary experiments conducted by Brauer *et al.* In these experiments simultaneous *in situ* small and large angle x-ray scattering measurements were made. The dynamics of the small angle scattering intensity was very similar to Fig. 3 and exhibited a Porod tail.

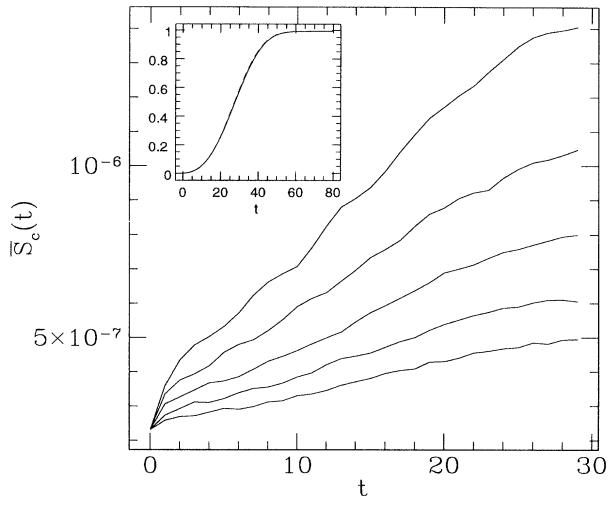

FIG. 3. S_c vs t for different wave numbers $q = 0.55$, 0.65, 0.75, 0.85, and 0.95 from bottom to top indicates two time regimes. Inset shows the ordered-phase fraction (dashed line) is well fit by Kolmogorov form (solid line).

This work was supported by the Natural Sciences and Engineering Research Council of Canada, and *le Fonds pour la Formation de Chercheurs et l'Aide à la Recherche du Québec*. K. R. E. acknowledges the support of Grant No. NSF-DMR-89-20538, administered through the University of Illinois Materials Research Laboratory.

[1] S. Brauer, Ph. D. thesis, McGill University, 1992; S. Brauer, H. E. Fischer, J. O. Ström-Olsen, M. Sutton, A. Zaluska, and G. B. Stephenson, Phys. Rev. B **47**, 11 757 (1993).

[2] B. Morin, Ph. D. thesis, McGill University, 1993.

[3] S. M. Allen and J. W. Cahn, Acta Metall. **23**, 1017 (1975); **24**, 425 (1976). See also L.-Q. Chen and W. Yang, Phys. Rev. B **50**, 15 752 (1994); L.-Q. Chen, Scrip. Metall. **32**, 115 (1995); J. A. Warren, W. C. Carter, and A. R. Roosen (unpublished).

[4] P. C. Hohenberg and B. I. Halperin, Rev. Mod. Phys. **49**, 435 (1977).

[5] Alternatively, one could include elastic stress and strain interactions. That description is complicated, so we use a simpler model which incorporates the essential features.

[6] M. E. Einhorn, R. Savit, and E. Rabinovici, Nucl. Phys. **B170**, 16 (1980).

[7] K. R. Elder, B. Morin, M. Grant, and R. C. Desai, Phys. Rev. B **44**, 6673 (1991).

[8] G. Porod, in *Small Angle X-Ray Scattering,* edited by O. Glatter and O. Kratsky (Academic, New York, 1982).

[9] Variables have been rescaled as $t \to [1/(\Gamma r)]t$, $\mathbf{x} \to (\kappa/r)^{1/2}\mathbf{x}$, $\vec{\psi} \to (r/v)^{1/4}\vec{\psi}$, $c \to (r/v)^{1/4}(r/w)^{1/2}c$, $\eta_\psi \to \Gamma r(r/v)^{1/4}\eta_\psi$, and $\eta_c \to \Gamma r(r/v)^{1/4}(r/w)^{1/2}\eta_c$, and parameters as $s \to (\sqrt{v/r})s$, $\alpha \to [(v/r)^{1/4}\sqrt{wr}]\alpha$, $D \to (\Gamma\kappa/w)D$, $\beta \to (w\kappa/r)\beta$, and $T \to [r(\kappa/r)^{d/2}\sqrt{r/v}]T$.

[10] J. D. Gunton, M. San Miguel, and P. Sahni, in *Phase Transitions and Critical Phenomena,* edited by C. Domb and J. L. Lebowitz (Academic Press, London, 1983), Vol. 8, p. 267; J. D. Gunton and M. Droz, *Introduction to the Theory of Metastable and Unstable States* (Springer-Verlag, Berlin, 1983).

[11] We do not expect the $1/q^{d+1}$ tail to be observed near the Bragg peak of a powder due to the orientational distribution of crystallites. [M. Grant and M. Sutton (unpublished)].

[12] A. N. Kolmogorov, Bull. Acad. Sci., USSR, Phys. Ser. **3**, 335 (1938).

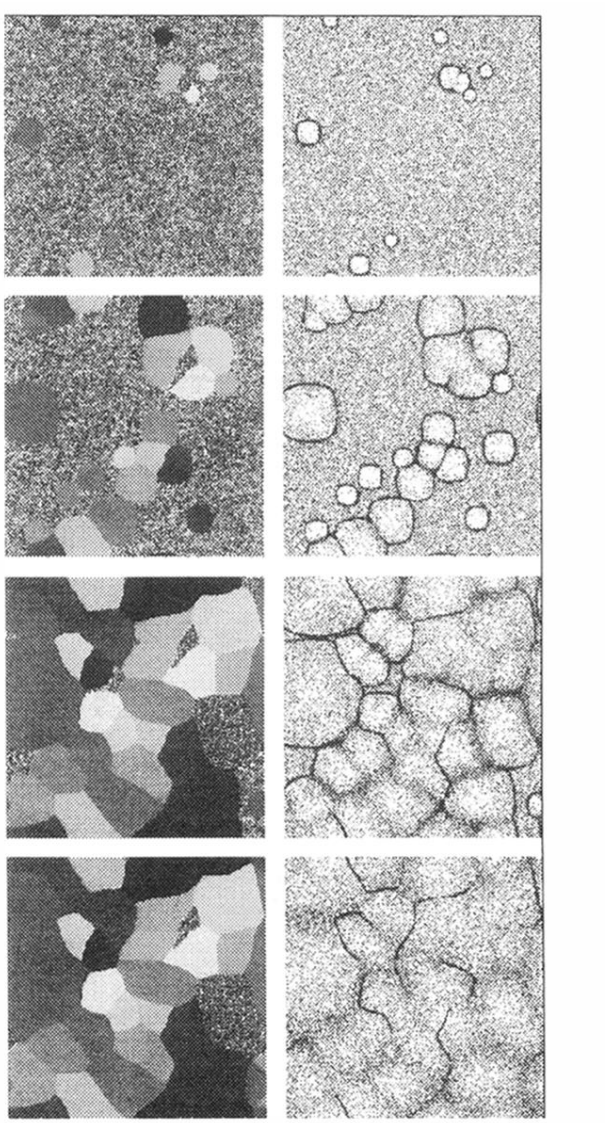

FIG. 1. Two parallel sets of configurations imaging the local magnitude of order parameter $|\vec{\psi}|$ (left) and the local concentration c (right) as a function of time $t = 8$, 24, 48, 80, from top to bottom. Gray scale of concentration shows weak step function in bulk crystallites due to differences in domain-wall energy. Also note the large concentration differences at different types of domain walls.